Computational Materials Science 204 (2022) 111134

Contents lists available at ScienceDirect

Computational Materials Science

journal homepage: www.elsevier.com/locate/commatsci

Exchange interaction between the high spin Co^{3+} states in $LaCoO_3$

Yu.S. Orlov [a,b,*], S.V. Nikolaev [a,b], V.A. Gavrichkov [b], S.G. Ovchinnikov [a,b]

[a] Siberian Federal University, 660041, Krasnoyarsk, Russia
[b] Kirensky Institute of Physics, Federal Research Center KSC SB RAS, 660036, Krasnoyarsk, Russia

ARTICLE INFO

Keywords:
Exchange interaction
Spin-orbital interaction
Magnetic phase diagram
Antiferromagnetism
Ferromagnetism
Hubbard model

ABSTRACT

The formation of the exchange interaction between HS Co^{3+} ions, which are excited in $LaCoO_3$, is studied within the multielectron approach. Two main contributions appear to be antiferromagnetic (AFM) and ferromagnetic (FM). When the ground state is LS, the total interaction is AFM. The crossover to the HS state may result in the FM ordering. The mean-field magnetic phase diagrams on the plane spin gap-temperature have been calculated without and with spin-orbital interaction in the HS term. Without spin-orbital interaction the reentrant magnetic order is possible. The spin-orbital coupling removes the reentrant phase transition and stabilizes the LS state. For known from experimental data values of the spin gap and exchange interaction, the ideal stoichiometric $LaCoO_3$ is very close to the LS–HS crossover and magnetic ordering border. The violations of local coordination and symmetry of the Co^{3+}-oxygen complexes that take place in the intergrain boundaries, at the surface of single crystals, and in the thin films on the strained substrate, may result in the formation of the HS state and FM order for such materials.

1. Introduction

Unique properties of undoped $LaCoO_3$ with a Co^{3+} ion low spin (LS) ground state and thermally induced spin-states and semiconductor–metal transitions have attracted much interest and attention [1–3]. At low temperature, a non-magnetic LS state with $S = 0$ determines the absence of magnetic moments in the bulk of the stoichiometric sample. There are two magnetic contributions, revealed by a Curie–Weiss paramagnetic susceptibility below 35 K that was ascribed to impurities [4] or to localized spins associated with the surface defects of the crystal lattice [2,5]. Similar behavior was observed also in $PrCoO_3$ and $NdCoO_3$ at rather high temperatures [6]. There are several reports on the ferromagnetic order in $LaCoO_3$. Hysteresis in the magnetization at $T = 1.9$ K has been found in precipitated powders and a single crystal as well [7]. Later two ferromagnetic (FM) phases with $T_c < 10$ K and with 20 K $< T_c <$ 100 K were obtained in coprecipitation derived $LaCoO_3$ powders [8]. In single crystals, a ferromagnetic component with $T_c \sim 85$ K has been observed [9] with a possible explanation by stabilization of the magnetic Co^{3+} states at the sample surface due to the different coordination of cations vs bulk states. A similar FM order at the surface of $LaCoO_3$ single crystal has been revealed by SQUID measurements below 85 K [10]. Also, FM order was found in epitaxially strained thin films [10–16]. The FM order was attributed to a tensile strain in a substrate. Recently, the FM order has been found in the interdiffusion region of compressively strained superlattices $LaCoO_3$ / $LaMnO_3$ [17].

That is why a study of the exchange interaction between magnetic ions in $LaCoO_3$ is of interest. Previously it was introduced as a fitting parameter to analyze the magnetization and the electron paramagnetic resonance measurements in a strong magnetic field up to 33 T [18]. The fitting of magnetization vs temperature dependences at different field values results in the antiferromagnetic (AFM) exchange interaction $J = 27.5$ K [18].

The ground state of $LaCoO_3$ is a nonmagnetic insulator with a low-spin (LS, $S = 0$) state of the Co^{3+} ion with t_{2g}^6 electronic configuration in the crystal field of the O_6 octahedron. A transition to the paramagnetic state occurs in the vicinity of $T = 100$ K, which is evident from the sharp increase in the magnetic susceptibility. However, the spin state of Co^{3+} ions above $T = 100$ K remains a mystery for a long time. According to the Tanabe–Sugano diagrams, for the d^6-ion with a change in the crystal field, a crossover between the LS and HS terms is possible. In the framework of the standard model of an ion in a crystal field, the energy of the IS state is so much higher than that for the LS and HS states that thermal population of it is out of the question.

Numerous and most modern studies have not yet provided unambiguous evidence in favor of the realization of the IS or HS state in the intermediate temperature range. We will provide references to works that are quite important in our opinion in favor of the IS- [19–24] and HS- [18,25–29] states. In our works and in this one, we adhere to the scenario in which the HS-state acts as the first excited state. In our opinion, this particular scenario is the most attractive lately.

* Corresponding author at: Siberian Federal University, 660041, Krasnoyarsk, Russia.
E-mail address: jso.krasn@mail.ru (Yu.S. Orlov).

https://doi.org/10.1016/j.commatsci.2021.111134
Received 2 October 2021; Received in revised form 8 December 2021; Accepted 9 December 2021
Available online 13 January 2022

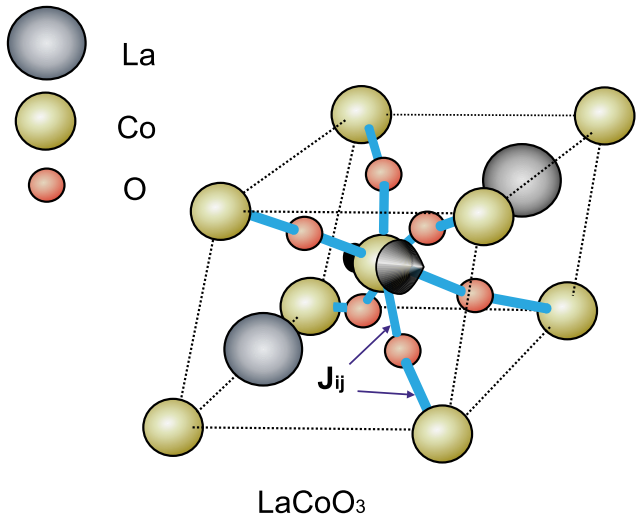

Fig. 1. Atomic structure of $LaCoO_3$. The 180° superexchange pathways Co^{3+}-Co^{3+} are shown in blue.

In this paper, we calculate the interatomic exchange interaction between the high spin (HS) terms of $LaCoO_3$ (Fig. 1). These terms are excited and not occupied in the ground state of the ideal stoichiometric crystal. Nevertheless, they may be occupied in the excited state at finite temperature or under external irradiation. HS terms may be the ground state at the surface or close to defects like the oxygen vacancy. We use the multielectron approach [30] that presents the total interatomic superexchange interaction as a sum of partial contributions from all cation terms, both the ground and excited ones. For example, the low spin (LS) terms of the Fe^{3+} ion with a ferromagnetic interatomic exchange are excited at low pressure in $FeBO_3$ and are stabilized above the spin crossover pressure, this ferromagnetic interaction is predicted to change the magnetic order in the LS phase [31]. The other example is given by a change of the exchange interaction sign in $FeBO_3$ under resonant optical pumping with d–d excitation from the HS Fe^{3+} term with $S = 5/2$ into the intermediate spin state with $S = 3/2$ [32]. Our multielectron approach is a generalization of the projection operator approach [33] to the Anderson-superexchange interaction calculation. We derive the expression for the superexchange interaction between two ions in the excited HS states, it is a sum of FM and AFM contributions. Depending on the ratio J_H/U_{eff}, where J_H is the intra-atomic Hund coupling and U_{eff} is the effective Hubbard parameter, the resulting interaction may be either FM or AFM. We also estimate possible magnetic ordering temperatures induced by oxygen vacancies.

The rest of the paper is organized as follows. The superexchange interaction between the high spin ions Co^{3+} $\left({}^5T_2\right)$ is considered in Section 2. The mean-field phase diagram of $LaCoO_3$ in the plane (spin gap, temperature) is discussed in Section 3. Section 4 contains the discussion of results.

2. Superexchange interaction between the high spin ions Co^{3+} $\left({}^5T_2\right)$

The DFT based approach to calculate the exchange parameter in the effective Heisenberg model has been developed for metals and alloys [34]. For $LaCoO_3$ as well to the Mott–Hubbard insulators such *ab initio* approach cannot be applied, because it does not treat strong electron correlations adequately. Recently its extension to strongly correlated systems has been developed [35]. Nevertheless, this extension is restricted by the effective s-d model and cannot be applied to $LaCoO_3$. More simple versions like LSDA+U [36,37] were used to study the superexchange interaction in strained $LaCoO_3$. These authors can reproduce FM coupling with increasing tensile strain, but the main features of $LaCoO_3$ physics with the temperature driven spin-state transition and semiconductor–metal transition under heating cannot be described by the DFT+U approach. Interesting results are shown by the quantum Monte Carlo method [38], but it are limited by the framework of the ground state of a magnetic material and are in the development stage. That is why we use in this paper the multielectron approach to the superexchange interaction [30], that allows to treat partial contributions from each excited term. This method allows treating the magnetism not only in the ground state, but also under optical pumping [32] and external pressure [39].

The calculation starts within the multi-band Hubbard model. By the unitary transformation similar to a conventional Hubbard model [33] we exclude the interband and interatomic virtual excitations in the second-order perturbation theory and obtain the effective Hamiltonian that operates in the electroneutral subspace of the Gilbert space (here it is d^6 subspace)

$$H_s = E_{LS}\sum_i X_i^{S,S} + E_{HS}\sum_{i,m} X_i^{m,m} + \sum_{i,j} J_{i,j}\vec{S}_i\vec{S}_j. \tag{1}$$

The first and the second terms describe the singlet LS and the HS with $S = 2$ and spin projections $m = (-2,-1,0,1,2)$, and the last term gives the superexchange interaction between the HS terms, spin operator for $S = 2$ in the representation of the Hubbard operators $X_i^{m,n} = |m\rangle\langle n|$ has the following components [40]

$$S_i^+ = 2X_i^{-1,-2} + \sqrt{6}X_i^{0,-1} + \sqrt{6}X_i^{+1,0} + 2X_i^{+2,+1},$$
$$S_i^- = (S_i^+)^\dagger,$$
$$S_i^z = 2X_i^{+2,+2} + X_i^{+1,+1} - X_i^{-1,-1} - 2X_i^{-2,-2}$$

According to the projection operator approach [30–33], to calculate the superexchange interaction we have considered the relevant multielectron terms in three sectors of the Hilbert space (Fig. 2). The electroneutral states with d^6 configuration include LS and HS terms, the electron addition states with d^7 configuration and the electron removal (hole addition) states with the d^5 configuration have different HS, LS, and intermediate spin (IS) terms, shown in Fig. 2. The superexchange interaction results from virtual electron–hole creation and annihilation shown in Fig. 2 by the exchange loops. Within the Hubbard projection operator technique, it is possible to separate each partial contribution to the total superexchange. The LS d^6 terms with $S = 0$ do not participate in the interatomic exchange. It is formed by the excited HS states (IS d^6 term lies higher in energy and its contribution to the total superexchange is not considered in this paper). This mechanism of the superexchange interaction is similar to the well-known in the Hubbard model Anderson superexchange interaction $J = 2t^2/U$. The novelty of the projection operator approach [30–32] is the possibility to separate different contributions.

Fig. 2(a) shows the virtual hole creation and annihilation at site i, in this process the initial d^6 HS lost the t_{2g} electron with the formation of the virtual d^5 HS term, then this electron comes back. At the same time, a neighbor site j gets an extra electron with the formation of the d^7 HS term ${}^4T_1$, after electron annihilation the HS d^6 term forming back. The considered in Fig. 2(a) exchange loop via t_{2g} π-bonding results in the ferromagnetic interatomic interaction

$$J^{FM}_{{}^6A,{}^4T_1} \approx -\frac{t_\pi^2}{\Delta\left({}^6A,{}^4T_1\right)}, \tag{2}$$

here t_π is the parameter of the cation–anion–cation π-hopping, the effective Hubbard U for this particular loop is given by the energy difference of the two final and two initial states

$$\Delta\left({}^6A,{}^4T_1\right) = \epsilon_e + \epsilon_h - 2\epsilon_0, \tag{3}$$

where

$$\epsilon_e = \epsilon\left({}^4T_1\right) = -8Dq + 21U - 11J_H,$$

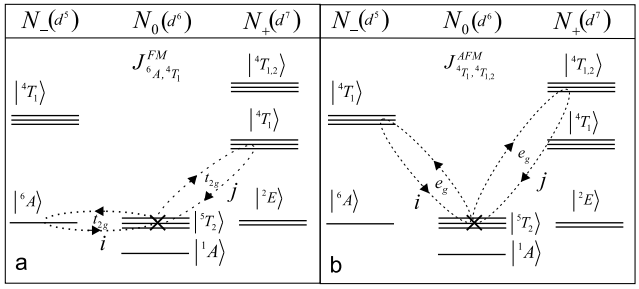

Fig. 2. Two exchange loops, corresponding to different virtual electron–hole excitations, that result in the ferromagnetic (a) and the antiferromagnetic (b) superexchange interaction between the excited high spin Co^{3+} ions.

$$\epsilon_h = \epsilon\left({}^6A\right) = 10\left(U - J_H\right),$$
$$\epsilon_0 = \epsilon\left({}^5T_2\right) = -4Dq + 15U - 10J_H.$$

Here $10Dq$ is the cubic crystal field, J_H is the intra-atomic Hund exchange parameter, and U is the effective intra-atomic Coulomb interaction value. We did not introduce two different parameters for the intraorbital and interorbital Coulomb interactions just for simplicity. Finally, we obtain

$$\Delta\left({}^6A, {}^4T_1\right) = U - J_H. \tag{4}$$

According to the general rules formulated in [30,31,39], when the spin values of the hole and electron virtual states are different (5/2 and 3/2 for the loop in Fig. 2(a)), the sign of interaction corresponds to a ferromagnetic coupling. When the spin values of the electron and hole virtual states are equal, the superexchange interaction is antiferromagnetic. Previously the same rules have been formulated for the exchange interaction between cations in the ground state [41,42].

Due to a small e_g-t_{2g} overlapping, we neglect such contribution to the effective Hamiltonian for the 180° exchange. The next relevant contribution involves e_g-e_g σ-bonding (Fig. 2(b)), both hole and electron virtual states have equal spin $S = 3/2$ values, so the AFM contribution is equal to

$$J^{AFM}_{^4T_1,^4T_{1,2}} \approx \frac{t_\sigma^2}{\Delta\left({}^4T_1, {}^4T_{1,2}\right)}, \tag{5}$$

where

$$\Delta\left({}^4T_1, {}^4T_{1,2}\right) = \epsilon_e + \epsilon_h - 2\epsilon_0,$$
$$\epsilon_e = \epsilon\left({}^4T_{1,2}\right) = 2Dq + 21U - 11J_H,$$
$$\epsilon_h = \epsilon\left({}^4T_1\right) = -10Dq + 10U - 6J_H,$$
$$\epsilon_0 = \epsilon\left({}^5T_2\right) = -4Dq + 15U - 10J_H.$$

Thus

$$\Delta\left({}^4T_1, {}^4T_{1,2}\right) = U + 3J_H.$$

For 180° exchange we can estimate the total superexchange interaction.

Let the hopping parameters $t_\sigma = t, t_\pi = t/3$, then the total AFM interaction is equal to

$$J = \frac{1}{2}\left(\frac{t^2}{U + 3J_H} - \frac{t^2/9}{U - J_H}\right) = \frac{4t^2}{9}\frac{U - \frac{3}{2}J_H}{(U + 3J_H)(U - J_H)}. \tag{6}$$

We use the parameters set (a): $U = 4$ eV, $J_H = 0.8$ eV, and $t = 0.2$ eV as the typical for late transition metal oxides. With these parameters, $J = 2.43$ meV $= 28.2$ K. We can compare this value with $J = 27.5$ K found from fitting the electron paramagnetic resonance data for $LaCoO_3$ in the strong magnetic field [18]. For the discussion of the HS/LS properties of $LaCoO_3$ within two-band Hubbard model, the value of $U = 4J_H$ has been considered [43,44]. With this ratio the total AFM exchange parameter (6) is given by $J = 0.0085t^2/U$. It looks like a typical for the Hubbard model term t^2/U with a smaller prefactor due to partial compensation of the AFM exchange by the FM contribution. For the same $U = 4$ eV, Hund coupling $J_H = 1$ eV and hopping $t = 0.2$ eV, set (b), one finds the similar exchange parameter $J = 24.6$ K. Thus, at least qualitative agreement between different approaches is achieved.

The other comparison with the experimental data uses the Neel temperature for FeO, $T_N = 200$ K [45]. In FeO, the magnetic cation Fe^{2+} has the same HS d^6 configuration with $S = 2$. For our calculated value $J = 28.2$ K, set (a), the spin-wave theory results in the $T_N = JzS(S+1)/3C = 226$ K. Here $z = 6$ is the nearest neighbor number, and $C = 1.5$ is the Watson integral. For the parameters from the set (b) the Neel temperature is 197 K. Usually the spin wave theory gives higher critical temperature than the experimental value, thus the set (a) looks more realistic. Thus we may conclude that our calculated value of J for the excited HS states in $LaCoO_3$ is rather close to experimental data, and the AFM coupling is stronger than the FM one for the stoichiometric $LaCoO_3$ in the ground state.

Now we ask ourselves whether the FM contribution may win in this competition. From Eq. (6) it is clear that the sign inversion is possible when $U < 1.5J_H$, because of $U > J_H$ for sure. So the total interaction is AFM when $U > 1.5J_H$, and it is FM when $U < 1.5J_H$. Whether this sign change can be realized experimentally? The Hund coupling parameter is the intra-atomic one, and it hardly may vary under external conditions. The parameter U in the multi-band Hubbard model or multi-band p-d model appears as the effective parameter $U_{eff}(d^6) = E_0(d^7) + E_0(d^5) - 2E_0(d^6)$ [46] with the value changing at the spin crossover between HS and LS terms [47,48]. For the d^6 cations, the LS–HS crossover results in the U_{eff} decrease by $2J_H$ [49]. With $U(HS) = U - 2J_H$ the exchange coupling in the HS state can be written like

$$J_{HS} = \frac{4t^2}{9}\frac{U - 3.5J_H}{(U + J_H)(U - 3J_H)}. \tag{7}$$

From Eq. (7) it follows that in the HS state the AFM interaction takes place for $U/J_H < 3$ and $U/J_H > 3.5$, and the FM interaction will win for $3 < U/J_H < 3.5$. For the parameters set (a) the AFM interaction exists in both LS and HS states. Let us consider the set (c): $U = 3.4$ eV, $J_H = 1$ eV, $t = 0.2$ eV. For this set $J_{LS} = 25.5$ K is AFM and $J_{HS} = -11.7$ K is FM. This sign change of the superexchange interaction may be the reason for the stabilization of the FM phase in the epitaxially strained $LaCoO_3$ thin films discussed in the introduction. Possible stabilization of the Co^{3+} HS state at the sample surface or near crystal defects also may result in the appearance of the FM interaction for these states and may induce the FM order.

3. Possibility for magnetic order in $LaCoO_3$

Even for an ideal stoichiometric sample at finite temperature, there is an exponentially small concentration of the HS ions that are coupled antiferromagnetically. Let us start with a very simple estimation for the Neel temperature for the excited ions with a concentration n_{HS}. In the mean-field approach one may write (here $z = 6$ is the nearest neighbor number, D is the spin gap between HS and LS terms, g is the degeneracy factor)

$$T_N = \frac{1}{3}JzS(S+1)n_{HS} = 12Jn_{HS}$$
$$= 12Jg\frac{exp(-D/T_N)}{1 + gexp(-D/T_N)}. \tag{8}$$

For the typical values of $D = 150$ K and $J = 30$ K, two values for T_N can be easily found. For $g = 3$ these values are $T_{N1} \sim 1.7J$ and $T_{N2} \sim 7.3J$ with a reentrant magnetic phase at $T_{N1} < T < T_{N2}$. The value of $g = 3$ results from the spin-orbital splitting of the HS term (Fig. 3). Early the reentrant behavior has been obtained for the FeO with similar d^6 configuration and HS/LS interplay by the Monte Carlo simulation [50].

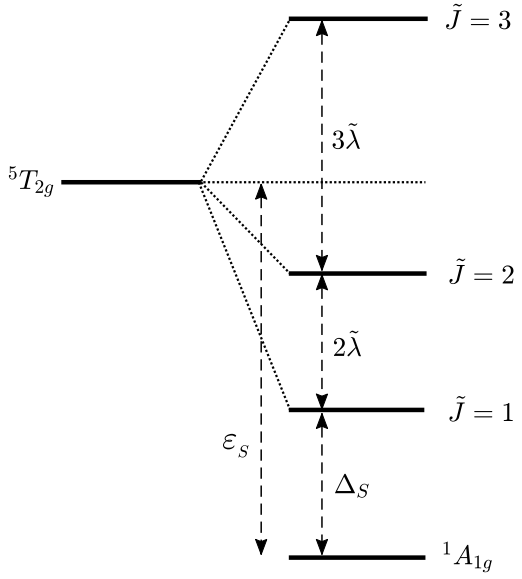

Fig. 3. Low-energy electronic structure of the Co^{3+} ion in $LaCoO_3$ originating from the $^5T_{2g}$ cubic subterm with the $^1A_{1g}$ singlet ground subterm put Δ_S below the lowest $^5T_{2g}$ state.

For more rigorous analysis we want to calculate the phase diagram and include a spin-orbital interaction within the HS state with $S = 2$ and pseudo orbital moment $L = 1$. In the mean-field (MF) approximation for the Hamiltonian (1), for two sublattices A and B we have

$$\begin{aligned}\hat{H}_S^{MF} &= Jzm_B\sum_{i_A}\hat{S}^z_{i_A} + Jzm_A\sum_{i_B}\hat{S}^z_{i_B}\\ &-Jz\sum_{i_A}\hat{n}_{i_A} - Jz\sum_{i_B}\hat{n}_{i_B}\\ &-\varepsilon_S\sum_{i_A}X^{s,s}_{i_A} - \varepsilon_S\sum_{i_B}X^{s,s}_{i_B}\\ &-\frac{1}{2}JzNm_Am_B + \frac{1}{2}JzN + NE_{HS},\end{aligned} \tag{9}$$

Here $m_{A(B)} = \left\langle \hat{S}^z_{i_{A(B)}} \right\rangle$ is the magnetization of sublattice A (B); the spin gap ε_S is the difference $E_{HS} - E_{LS}$.

Ropka and Radwanski [51] provide the proof for the ^5D term origin of an excited triplet observed in the electron-spin-resonance (ESR) experiments by Noguchi et al. [25]. They have succeeded to fully describe experimental ESR results both for the zero-field g-factor, of 3.35, and the splitting D of 4.90 cm^{-1}, as well as for the magnetic field applied along with different crystallographic directions within the localized electron atomic-like approach as originating from excitations within the lowest triplet of the $^5T_{2g}$ octahedral subterm of the ^5D term. In their atomic-like approach the d electrons of the Co^{3+} ion in $LaCoO_3$ form the highly-correlated atomic-like $3d^6$ system with the singlet $^1A_{1g}$ ground state (an octahedral subterm of the ^1I term) and the excited octahedral $^5T_{2g}$ subterm of the ^5D term. The ESR experiment can be taken as confirmation of the existence of the discrete electronic structure for $3d$ electron states in $LaCoO_3$ on the meV scale.

For the description of the excited HS state in $LaCoO_3$ and its magnetic properties we apply the Hamiltonian

$$\hat{H}_{eff}^{MF} = \hat{H}_S^{MF} + \hat{H}_{LS} + \hat{H}_{cub} + \hat{H}_{trigonal}, \tag{10}$$

where

$$\hat{H}_{LS} = \tilde{\lambda}\tilde{\vec{L}}\vec{S} = \tilde{\lambda}\left(\tilde{L}_zS_z + \frac{1}{2}\tilde{L}_+S_- + \frac{1}{2}\tilde{L}_-S_+\right),$$
$$\hat{H}_{cub} = -\frac{2}{3}B_4\left(O_4^0 - 20\sqrt{2}O_4^3\right)$$

Table 1
The eigenstates of $\hat{H}_{LS} + \hat{H}_{cub}$ classified by irreducible representations of O_h group. The basis functions $|\tilde{J}, m_{\tilde{J}}\rangle$ are listed in Table 2.

$\tilde{J}=1$	$\|T_1,1\rangle = \|1,1\rangle$ $\|T_1,0\rangle = \|1,0\rangle$ $\|T_1,-1\rangle = \|1,-1\rangle$
$\tilde{J}=2$	$\|E,\theta\rangle = \|2,0\rangle$ $\|E,\varepsilon\rangle = \frac{1}{\sqrt{2}}\|2,2\rangle + \frac{1}{\sqrt{2}}\|2,-2\rangle$ $\|T_2,1\rangle = \|2,+1\rangle$ $\|T_2,0\rangle = \frac{1}{\sqrt{2}}\|2,2\rangle - \frac{1}{\sqrt{2}}\|2,-2\rangle$ $\|T_2,-1\rangle = \|2,-1\rangle$
$\tilde{J}=3$	$\|A_2,a_2\rangle = \frac{1}{\sqrt{2}}\|3,2\rangle - \frac{1}{\sqrt{2}}\|3,-2\rangle$ $\|T_1,1\rangle = -\frac{\sqrt{5}}{2\sqrt{2}}\|3,-3\rangle - \frac{\sqrt{3}}{2\sqrt{2}}\|3,1\rangle$ $\|T_1,0\rangle = \|3,0\rangle$ $\|T_1,-1\rangle = -\frac{\sqrt{5}}{2\sqrt{2}}\|3,3\rangle - \frac{\sqrt{3}}{2\sqrt{2}}\|3,-1\rangle$ $\|T_2,1\rangle = -\frac{\sqrt{3}}{2\sqrt{2}}\|3,3\rangle + \frac{\sqrt{5}}{2\sqrt{2}}\|3,-1\rangle$ $\|T_2,0\rangle = \frac{1}{\sqrt{2}}\|3,2\rangle + \frac{1}{\sqrt{2}}\|3,-2\rangle$ $\|T_2,-1\rangle = -\frac{\sqrt{3}}{2\sqrt{2}}\|3,-3\rangle + \frac{\sqrt{5}}{2\sqrt{2}}\|3,1\rangle$

is the cubic crystal-field Hamiltonian for the z-axis along with the cube diagonal and O_m^n are the Stevens operators collected in, e.g. [52]. This form is useful for $LaCoO_3$ due to the experimentally observed rhombohedral (trigonal) distortion that can be then described by the parameter B_2^0, $\hat{H}_{trigonal} = B_2^0O_2^0$. The energy states, calculated for the dominant octahedral crystal field, weaker intra-atomic spin–orbit interactions, are shown in Fig. 3.

The energy levels in Fig. 3 are given by

$$\varepsilon_S = E_{HS} - E_{LS} = \left(E_{LS} + \Delta_S + 3\tilde{\lambda}\right) - E_{LS} = \Delta_S + 3\tilde{\lambda},$$
$$E_{\tilde{J}=1} = E_{LS} + \Delta_S,$$
$$E_{\tilde{J}=2} = E_{LS} + \Delta_S + 2\tilde{\lambda},$$
$$E_{\tilde{J}=3} = E_{LS} + \Delta_S + 5\tilde{\lambda}$$

with the spin-orbital coupling $\tilde{\lambda} = 185$ K.

Solving the problem on the eigenvalues

$$\hat{H}_{eff}^{MF}|\psi\rangle_k = E_k|\psi\rangle_k, \tag{11}$$

where $|\psi\rangle_k = \sum_l C_{kl}|\varphi\rangle_l$ are the eigenstates of Hamiltonian (10), and using the solutions corresponding to the minimum free energy $F = -k_BT\ln Z$, with the partition function $Z = \sum_k \exp\left(-\frac{E_k}{k_BT}\right)$, we can found

$$\begin{aligned}m_{A(B)} &= \left\langle \hat{S}^z_{i_{A(B)}} \right\rangle\\ &= Z^{-1}\sum_k \exp\left(-\frac{E_k}{k_BT}\right)\left\langle \psi_k \left| \hat{S}^z_{i_{A(B)}} \right| \psi_k \right\rangle\\ n^{LS(HS)}_{i_{A(B)}} &= \left\langle \hat{n}^{LS(HS)}_{i_{A(B)}} \right\rangle\\ &= Z^{-1}\sum_k \exp\left(-\frac{E_k}{k_BT}\right)\left\langle \psi_k \left| \hat{n}^{LS(HS)}_{i_{A(B)}} \right| \psi_k \right\rangle\end{aligned}$$

The eigenfunctions $|\varphi\rangle_l$ of $\hat{H}_{LS} + \hat{H}_{cub}$ are listed in Table 1. For simplicity the rhombohedral (trigonal) distortion is not considered, $B_2^0 = 0$.

We start with the phase diagrams without spin-orbital coupling. Fig. 4 demonstrates the magnetization (a) and population of the HS state (b) at $J = 28$ K, $z = 6$ and $\tilde{\lambda} = 0$ in the coordinates temperature T-spin gap Δ_S. Hereinafter, the temperature and spin gap are given in terms of exchange parameter J. It can be seen that, due to the presence of the cooperative exchange coupling J, the ground magnetically ordered HS state is preserved in a system up to $\Delta_S = \Delta_S^c \approx 7.5J$ (Fig. 4(a), (b)), although in the single-ion picture the LS state is ground at $\Delta_S > 0$. The growth of the critical value Δ_S^c due to the cooperative effects is quite clear since the exchange coupling stabilizes the HS state via lowering its energy. At $\Delta_S > \Delta_S^c$, the ground magnetic HS state

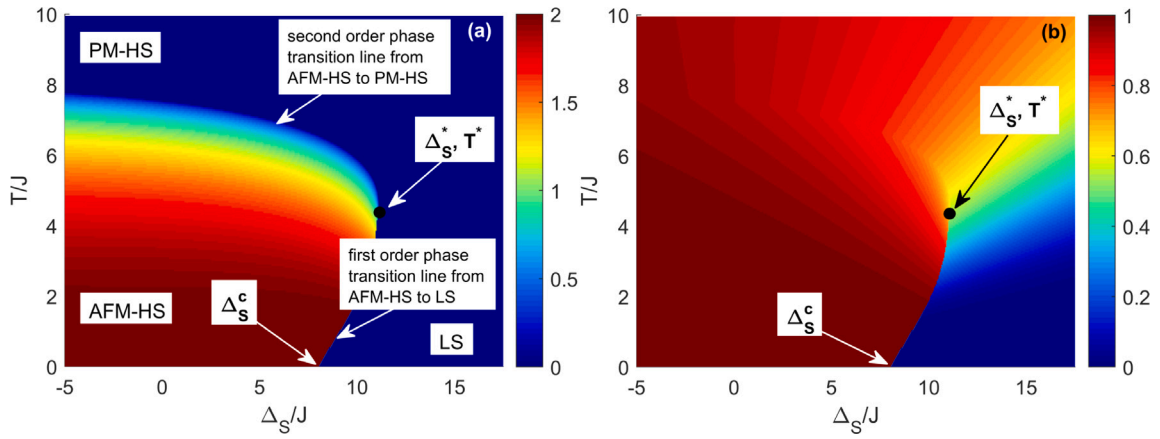

Fig. 4. Phase diagrams of (a) the magnetization and (b) populations of the HS state at $J = 28$ K, $z = 6$ and $\tilde{\lambda} = 0$.

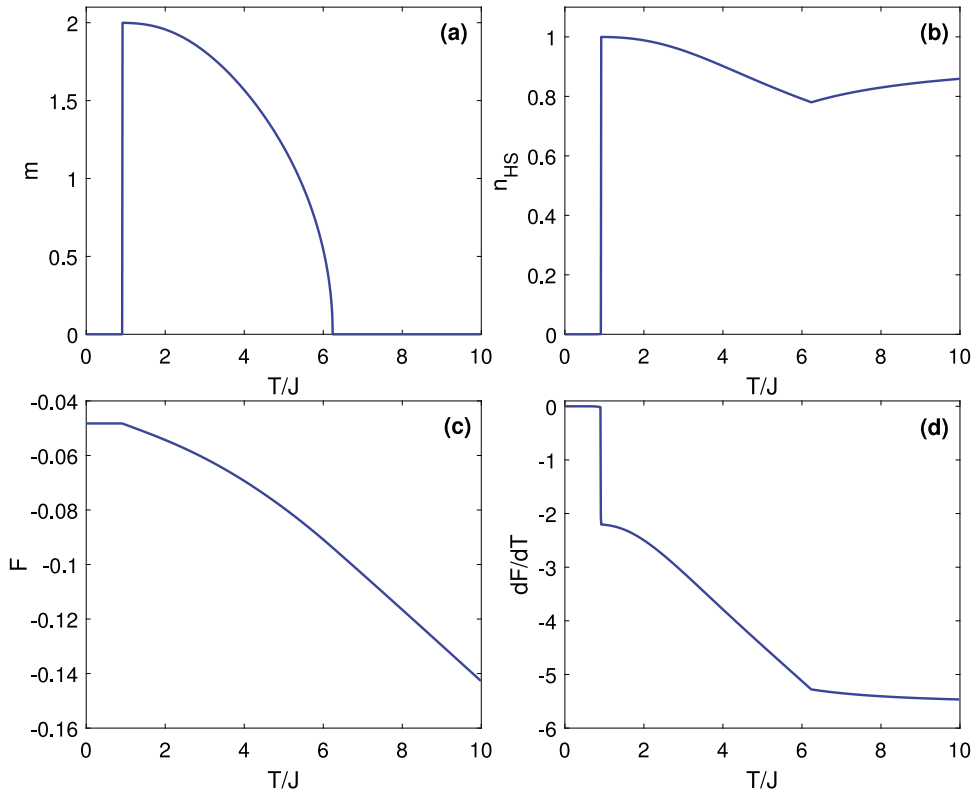

Fig. 5. Temperature dependences of (a) magnetization, (b) population of the HS state, (c) minimum free energy, and its temperature derivative (d) at $\Delta_S/J = 9$ ($J = 28$ K, $z = 6$ and $\tilde{\lambda} = 0$).

changes for the nonmagnetic LS state (Fig. 4(a), (b)). In the range of $\Delta_S < \Delta_S^c$ (Fig. 4(a), (b)), with increasing temperature, the system undergoes a second-order phase transition from the magnetic HS to the HS paramagnetic state. If $\Delta_S^c < \Delta_S < \Delta_S^*$, the system firstly undergoes a first-order transition from the nonmagnetic LS to the HS-AFM state and then a second-order phase transition from the HS-AFM to the HS paramagnetic state. This is the area of a reentrant transition discussed in the beginning of Section 3. In the diagram, one can clearly see the existence of a tricritical point (T^* and Δ_S^* in Fig. 4(a), (b)), at which the line of the second-order phase transitions continuously passes to the line of the first-order ones.

Fig. 5 shows as an example the temperature dependencies of (a) magnetization, (b) population of the HS state, (c) minimum free energy, and its temperature derivative (d) at $\Delta_S/J = 9$ in the reentrant area.

Reentrant transition is evident from Fig. 5 with the nonmagnetic LS below $T/J < 0.91$, the HS AFM phase between $0.91 < T/J < 6.24$, and the HS paramagnetic phase above $T/J = 6.24$. The LS nonmagnetic phase is stable for all temperatures above the critical point Δ_S^*.

Fig. 6 shows the effect of the spin-orbital interaction on the phase diagrams of the magnetization (a) and population of the HS state (b) at $J = 28$ K, $z = 6$ and $\tilde{\lambda} = 185$ K. The white dashed line corresponds to $LaCoO_3$.

The effect of spin-orbital interaction is crucial. It removes the reentrant behavior and decreases the stability area of the HS state. Instead of the spin crossover point at the spin gap $7.5J$ in Fig. 4, the same point is about $5.3J$ in Fig. 6. With the spin gap for $LaCoO_3$ $\Delta_S = 150$ K and $J = 28$ K [18,51] the ratio $\Delta_S/J = 5.36$. This point corresponding to $LaCoO_3$ in Fig. 6 is marked by the white dashed vertical line. Thus, we conclude that $LaCoO_3$ may be called a system in proximity to magnetic order and to crossover in the HS state. According to the Tanabe–Sugano diagrams, the intersection of the LS- and HS-states occurs at a crystal

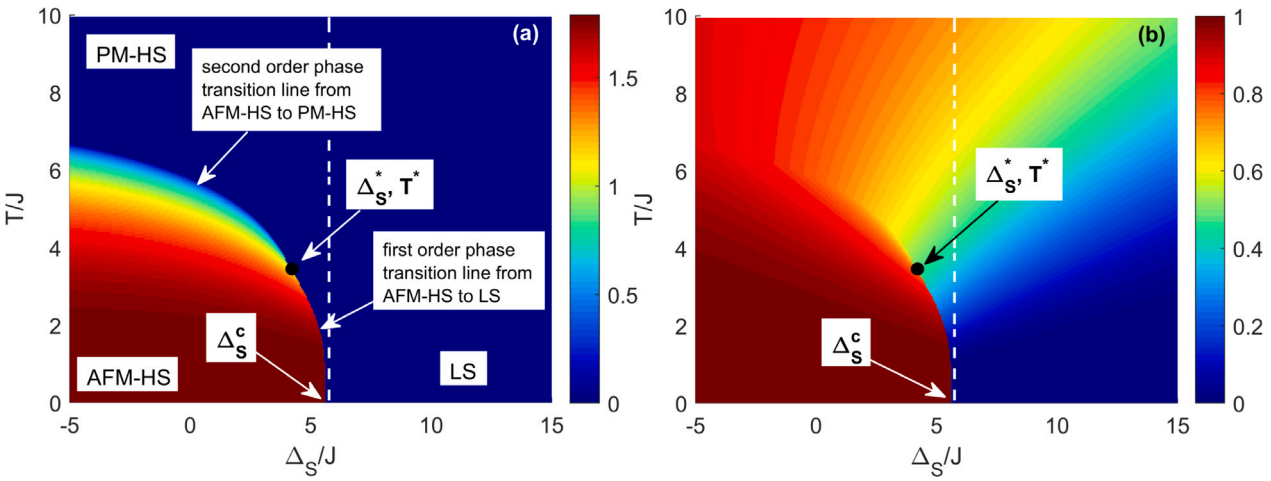

Fig. 6. Phase diagrams of (a) the magnetization and (b) populations of the HS state at $J = 28$ K, $z = 6$ and $\tilde{\lambda} = 185$ K. The white dashed line corresponds to $LaCoO_3$.

Table 2
The eigenstates of $\hat{H}_{LS}$ represented in basis of HS states $|\tilde{l}, S_z\rangle$, where $\tilde{l} = \pm 1, 0$ denotes the projection of the effective orbital angular momentum and $S_z = \pm 2, \pm 1, 0$ denotes the spin projection.

$\|\tilde{J}=1,0\rangle = \sqrt{\frac{2}{5}}\|\tilde{0},0\rangle - \sqrt{\frac{3}{10}}\|+\tilde{1},-1\rangle - \sqrt{\frac{3}{10}}\|-\tilde{1},+1\rangle$
$\|\tilde{J}=1,\pm1\rangle = \sqrt{\frac{1}{10}}\|\pm\tilde{1},0\rangle - \sqrt{\frac{3}{10}}\|\tilde{0},\pm1\rangle + \sqrt{\frac{3}{5}}\|\mp\tilde{1},\pm2\rangle$
$\|\tilde{J}=2,0\rangle = -\sqrt{\frac{1}{2}}\|+\tilde{1},-1\rangle + \sqrt{\frac{1}{2}}\|-\tilde{1},+1\rangle$
$\|\tilde{J}=2,\pm1\rangle = \frac{1}{\sqrt{2}}\|\pm\tilde{1},0\rangle - \frac{1}{\sqrt{6}}\|\tilde{0},\pm1\rangle - \frac{1}{\sqrt{3}}\|\mp\tilde{1},\pm2\rangle$
$\|\tilde{J}=2,\pm2\rangle = \frac{1}{\sqrt{3}}\|\pm\tilde{1},\pm1\rangle - \sqrt{\frac{2}{3}}\|\tilde{0},\pm2\rangle$
$\|\tilde{J}=3,0\rangle = -\sqrt{\frac{3}{5}}\|\tilde{0},0\rangle - \sqrt{\frac{1}{5}}\|+\tilde{1},-1\rangle - \sqrt{\frac{1}{5}}\|-\tilde{1},+1\rangle$
$\|\tilde{J}=3,\pm1\rangle = -\sqrt{\frac{2}{5}}\|\pm\tilde{1},0\rangle - \sqrt{\frac{8}{15}}\|\tilde{0},\pm1\rangle - \sqrt{\frac{1}{15}}\|\mp\tilde{1},\pm2\rangle$
$\|\tilde{J}=3,\pm2\rangle = -\sqrt{\frac{2}{3}}\|\pm\tilde{1},\pm1\rangle - \sqrt{\frac{1}{3}}\|\tilde{0},\pm2\rangle$
$\|\tilde{J}=3,\pm3\rangle = \|\pm\tilde{1},\pm2\rangle$

field of $10Dq \sim 2.6$ eV. At the same time, the spin gap in $LaCoO_3$ is $\Delta_S \sim 150$ K; therefore, a downward change in the crystal field by $\sim 0.5\%$ can stabilize the HS state relative to LS.

4. Discussions

We have found that the bulk ideal crystal of $LaCoO_3$ is very close to the border of the magnetic instability. Crossing this border in Fig. 6 results in the LS to HS crossover. According to our analysis of the competing AFM and FM contributions to the superexchange interaction (Eqs. (6), (7) and discussion in the end of Section 2), in the HS state the total exchange may be AFM or FM depending on the material parameters. For the FM sign it may explain the found experimentally FM order in three different type of $LaCoO_3$ samples [7–17]: FM in polycrystalline powders, at surfaces of bulk single crystals and in strained films. Due to the proximity of the bulk $LaCoO_3$ to the HS and magnetic order found in Fig. 6, small changed of the local symmetry or local interatomic distance in the intergrain boundaries of the powder samples, at the surface of a single crystal, and in the thin film under strained substrate may stabilize the FM order. Of course, these conclusions are only qualitative. Recently, the alternative approach to the ferromagnetism of $LaCoO_3$ films that originates from effective superexchange interactions between atoms in the high-spin (HS) state mediated by the intermediate-spin excitations has been studied in the paper [53].

Let us discuss the effect of the tensile strain on magnetic properties of $LaCoO_3$ films in more details. Besides the papers [10–16], discussed in the introduction, recently this effect has been demonstrate also in the epitaxial $LaCoO_3$ films [54,55]. Study of the magnetic anisotropy indicates that the ferromagnetism seems to be correlated to the tensile strain, i.e., larger strain for larger coercive field [56]. The LS and HS states of the Co^{3+} ion are separated by a spin gap $E_{HS} - E_{LS} = 2(10Dq - 2J_H)$ [47]. Here $10Dq$ is the crystal field parameter, which increases with the Co-O distance decrease (under external pressure) or decreases with the Co-O distance increase (under tensile strain). In $LaCoO_3$ the spin gap is small, about 0.01 eV [3,25,51], so the tensile strain may result in the sign inversion of the spin gap and stabilization of the HS magnetic moments which can demonstrate the FM order according our calculations. On the contrary, the external pressure stabilizes the LS state and cannot results in the magnetic order, according to the experimental data [56].

A similar effect of the spin crossover on the sign of the superexchange interaction has been discussed earlier for $FeBO_3$, where the Fe^{3+} HS state exists below the spin crossover pressure $P_s = 50$ GPa, and in the LS state above P_s, see the experimental phase diagram in [57]. This spin-crossover results in the sharp suppression of the U_{eff} from 4.2 eV below P_s till 1.4 eV above P_s [58]. Thus the condition $U > 3J_H$ is violated at the spin crossover. The direct calculation of the superexchange interaction in $FeBO_3$ within the same approach gives the conclusion of the AFM HS and FM LS states [31].

A new interesting experimental option is related with the time-resolved multidimensional photoemission spectroscopy, which was recently used to study ultrafast dynamics of Lifshitz transition [59]. It was found that under the dynamical pumping U depends on time and decreases. Thus in principle it is possible that the AFM state will transform into the FM state and then during the relaxation process the damping oscillations AFM/FM interactions may exist.

5. Conclusion

Within the multielectron approach, we have studied the formation of the exchange interaction between HS Co^{3+} ions, which are excited in $LaCoO_3$ in the ground state. Two main contributions appear to have opposite signs, one is antiferromagnetic and the other tends to ferromagnetism. When the ground state is LS, the total interaction between excited HS terms is AFM with the value of the total interaction parameter close to the known from experimental data. The crossover to the HS state may result in the FM ordering. The mean-field magnetic phase diagrams on the plane spin gap-temperature have been calculated without and with spin-orbital interaction in the HS term. Without spin-orbital interaction the reentrant magnetic order is possible with nonmagnetic LS ground state, that becomes AFM with heating in some temperature interval, and finally, the nonmagnetic HS state appears at high temperatures. The spin orbital coupling removes the reentrant phase transition and stabilizes the LS state. For known

from experimental data values of the spin gap and exchange interaction for $LaCoO_3$, the ideal stoichiometric composition is very close to the LS–HS crossover and magnetic ordering border. The violations of local coordination and symmetry of the Co-oxygen complexes that may take place in the intergrain boundaries, at the surface of single crystals, and in the thin films on the strained substrate, may result to the formation of the HS state and FM order for such materials.

CRediT authorship contribution statement

Yu.S. Orlov: Writing – review & editing. **S.V. Nikolaev:** Writing – review & editing. **V.A. Gavrichkov:** Writing – review & editing. **S.G. Ovchinnikov:** Writing – review & editing.

Declaration of competing interest

The authors declare that they have no known competing financial interests or personal relationships that could have appeared to influence the work reported in this paper.

Acknowledgment

We are thankful to the Russian Science Foundation, Russia for the financial support under the project 18-12-00022.

References

[1] J.B. Goodenough, Metallic oxides, Prog. Solid State Chem. 5 (1971) 145–399, http://dx.doi.org/10.1016/0079-6786(71)90018-5.
[2] M.A. Senaris-Rodriguez, J.B. Goodenough, $LaCoO_3$ revisited, J. Solid State Chem. 116 (2) (1995) 224–231, http://dx.doi.org/10.1006/jssc.1995.1207.
[3] N.B. Ivanova, S.G. Ovchinnikov, M.M. Korshunov, I.M. Eremin, N.V. Kazak, Specific features of spin, charge, and orbital ordering in cobaltites, Phys.-Usp. 52 (8) (2009) 789–810, http://dx.doi.org/10.3367/ufne.0179.200908b.0837.
[4] S. Yamaguchi, Y. Okimoto, Y. Tokura, Local lattice distortion during the spin-state transition in $LaCoO_3$, Phys. Rev. B 55 (14) (1997) R8666, http://dx.doi.org/10.1103/physrevb.55.r8666.
[5] S. Zhou, L. Shi, J. Zhao, L. He, H. Yang, S. Zhang, Ferromagnetism in $LaCoO_3$ nanoparticles, Phys. Rev. B 76 (17) (2007) 172407, http://dx.doi.org/10.1103/physrevb.76.172407.
[6] J.-Q. Yan, J.-S. Zhou, J.B. Goodenough, Bond-length fluctuations and the spin-state transition in $LCoO_3$ (L= La, Pr, and Nd), Phys. Rev. B 69 (13) (2004) 134409, http://dx.doi.org/10.1103/physrevb.69.134409.
[7] N. Menyuk, K. Dwight, P. Raccah, Low temperature crystallographic and magnetic study of $LaCoO_3$, J. Phys. Chem. Solids 28 (4) (1967) 549–556, http://dx.doi.org/10.1016/0022-3697(67)90085-6.
[8] J. Androulakis, N. Katsarakis, J. Giapintzakis, Ferromagnetic and antiferromagnetic interactions in lanthanum cobalt oxide at low temperatures, Phys. Rev. B 64 (17) (2001) 174401, http://dx.doi.org/10.1103/physrevb.64.174401.
[9] J.-Q. Yan, J.-S. Zhou, J.B. Goodenough, Ferromagnetism in $LaCoO_3$, Phys. Rev. B 70 (1) (2004) 014402, http://dx.doi.org/10.1103/physrevb.70.014402.
[10] A. Harada, T. Taniyama, Y. Takeuchi, T. Sato, T. Kyomen, M. Itoh, Ferromagnetism at the surface of a $LaCoO_3$ single crystal observed using scanning squid microscopy, Phys. Rev. B 75 (18) (2007) 184426, http://dx.doi.org/10.1103/physrevb.75.184426.
[11] D. Fuchs, C. Pinta, T. Schwarz, P. Schweiss, P. Nagel, S. Schuppler, R. Schneider, M. Merz, G. Roth, H.v. Lohneysen, Ferromagnetic order in epitaxially strained $LaCoO_3$ thin films, Phys. Rev. B 75 (14) (2007) 144402, http://dx.doi.org/10.1103/physrevb.75.144402.
[12] A. Herklotz, A.D. Rata, L. Schultz, K. Dorr, Reversible strain effect on the magnetization of $LaCoO_3$ films, Phys. Rev. B 79 (9) (2009) 092409, http://dx.doi.org/10.1103/physrevb.79.092409.
[13] V.V. Mehta, M. Liberati, F.J. Wong, R.V. Chopdekar, E. Arenholz, Y. Suzuki, Ferromagnetism in tetragonally distorted $LaCoO_3$ thin films, J. Appl. Phys. 105 (7) (2009) 07E503, http://dx.doi.org/10.1063/1.3059606.
[14] N. Biskup, J. Salafranca, V. Mehta, M.P. Oxley, Y. Suzuki, S.J. Pennycook, S.T. Pantelides, M. Varela, Insulating ferromagnetic $LaCoO_{3-\delta}$ films: A phase induced by ordering of oxygen vacancies, Phys. Rev. Lett. 112 (8) (2014) 087202, http://dx.doi.org/10.1103/physrevlett.112.087202.
[15] H. Liu, L. Shi, Y. Guo, S. Zhou, J. Zhao, C. Wang, L. He, Y. Li, Nature of ferromagnetic ordered state in $LaCoO_3$ epitaxial nano-thin film on $LaAlO_3$ substrate, J. Alloys Compd. 594 (2014) 158–164, http://dx.doi.org/10.1016/j.jallcom.2014.01.126.
[16] Q. Feng, D. Meng, H. Zhou, G. Liang, Z. Cui, H. Huang, J. Wang, J. Guo, C. Ma, X. Zhai, Q. Lu, Y. Lu, Direct imaging revealing halved ferromagnetism in tensile-strained $LaCoO_3$ thin films, Phys. Rev. Mater. 3 (7) (2019) 074406, http://dx.doi.org/10.1103/physrevmaterials.3.074406.
[17] L. Wu, M. Chen, C. Li, J. Zhou, L. Shen, Y. Wang, Z. Zhong, M. Feng, Y. Zhang, K. Han, T.V. Venkatesan, S.J. Pennycook, P. Yu, J. Ma, X.R. Wang, C.-W. Nan, Ferromagnetism and matrix-dependent charge transfer in strained $LaMnO_3$-$LaCoO_3$ superlattices, Mater. Res. Lett. 6 (9) (2018) 501–507, http://dx.doi.org/10.1080/21663831.2018.1482840.
[18] M.J.R. Hoch, S. Nellutla, J. van Tol, E.S. Choi, J. Lu, H. Zheng, J.F. Mitchell, Diamagnetic to paramagnetic transition in $LaCoO_3$, Phys. Rev. B 79 (21) (2009) 214421, http://dx.doi.org/10.1103/physrevb.79.214421.
[19] K. Asai, A. Yoneda, O. Yokokura, J. Tranquada, G. Shirane, K. Kohn, Two spin-state transitions in $LaCoO_3$, J. Phys. Soc. Japan 67 (1) (1998) 290–296, http://dx.doi.org/10.1143/JPSJ.67.290.
[20] T. Saitoh, T. Mizokawa, A. Fujimori, M. Abbate, Y. Takeda, M. Takano, Electronic structure and temperature-induced paramagnetism in $LaCoO_3$, Phys. Rev. B 55 (1997) 4257–4266, http://dx.doi.org/10.1103/PhysRevB.55.4257.
[21] R.F. Klie, J.C. Zheng, Y. Zhu, M. Varela, J. Wu, C. Leighton, Direct measurement of the low-temperature spin-state transition in $LaCoO_3$, Phys. Rev. Lett. 99 (2007) 047203, http://dx.doi.org/10.1103/PhysRevLett.99.047203.
[22] C. Zobel, M. Kriener, D. Bruns, J. Baier, M. Grüninger, T. Lorenz, P. Reutler, A. Revcolevschi, Evidence for a low-spin to intermediate-spin state transition in $LaCoO_3$, Phys. Rev. B 66 (2002) 020402, http://dx.doi.org/10.1103/PhysRevB.66.020402.
[23] C. Zobel, M. Kriener, D. Bruns, J. Baier, M. Grüninger, T. Lorenz, P. Reutler, A. Revcolevschi, Erratum: Evidence for a low-spin to intermediate-spin state transition in $LaCoO_3$ [Phys. Rev. B 66, 020402 (R)(2002)], Phys. Rev. B 71 (2005) 019902, http://dx.doi.org/10.1103/PhysRevB.71.019902.
[24] P.G. Radaelli, S.-W. Cheong, Structural phenomena associated with the spin-state transition in $LaCoO_3$, Phys. Rev. B 66 (2002) 094408, http://dx.doi.org/10.1103/PhysRevB.66.094408.
[25] S. Noguchi, S. Kawamata, K. Okuda, H. Nojiri, M. Motokawa, Evidence for the excited triplet of Co^{3+} in $LaCoO_3$, Phys. Rev. B 66 (9) (2002) 094404, http://dx.doi.org/10.1103/physrevb.66.094404.
[26] M.W. Haverkort, Z. Hu, J.C. Cezar, T. Burnus, H. Hartmann, M. Reuther, C. Zobel, T. Lorenz, A. Tanaka, N.B. Brookes, H.H. Hsieh, H.-J. Lin, C.T. Chen, L.H. Tjeng, Spin state transition in $LaCoO_3$ studied using soft X-ray absorption spectroscopy and magnetic circular dichroism, Phys. Rev. Lett. 97 (2006) 176405, http://dx.doi.org/10.1103/PhysRevLett.97.176405.
[27] A. Podlesnyak, S. Streule, J. Mesot, M. Medarde, E. Pomjakushina, K. Conder, A. Tanaka, M.W. Haverkort, D.I. Khomskii, Spin-state transition in $LaCoO_3$: Direct neutron spectroscopic evidence of excited magnetic states, Phys. Rev. Lett. 97 (2006) 247208, http://dx.doi.org/10.1103/PhysRevLett.97.247208.
[28] A. Podlesnyak, K. Conder, E. Pomjakushina, A. Mirmelstein, P. Allenspach, D. Khomskii, Effect of light Sr doping on the spin–state transition in $LaCoO_3$, J. Magn. Magn. Mater. 310 (2, Part 2) (2007) 1552–1554, http://dx.doi.org/10.1016/j.jmmm.2006.10.901, Proceedings of the 17th International Conference on Magnetism.
[29] M. Rotter, Z.-S. Wang, A.T. Boothroyd, D. Prabhakaran, A. Tanaka, M. Doerr, Mechanism of spin crossover in $LaCoO_3$ resolved by shape magnetostriction in pulsed magnetic fields, Sci. Rep. 4 (2014) 7003, http://dx.doi.org/10.1038/srep07003.
[30] V.A. Gavrichkov, S.I. Polukeev, S.G. Ovchinnikov, Contribution from optically excited many-electron states to the superexchange interaction in Mott-Hubbard insulators, Phys. Rev. B 95 (14) (2017) 144424, http://dx.doi.org/10.1103/physrevb.95.144424.
[31] V.A. Gavrichkov, S.I. Polukeev, S.G. Ovchinnikov, Superexchange interaction in magnetic insulators with spin crossover, J. Exp. Theor. Phys. 127 (4) (2018) 713–720, http://dx.doi.org/10.1134/s1063776118100023.
[32] R.V. Mikhaylovskiy, T.J. Huisman, V.A. Gavrichkov, S.I. Polukeev, S.G. Ovchinnikov, D. Afanasiev, R.V. Pisarev, T. Rasing, A.V. Kimel, Resonant pumping of d-d crystal field electronic transitions as a mechanism of ultrafast optical control of the exchange interactions in iron oxides, Phys. Rev. Lett. 125 (15) (2020) 157201, http://dx.doi.org/10.1103/physrevlett.125.157201.
[33] K.A. Chao, J. Spalek, A.M. Oles, Kinetic exchange interaction in a narrow s-band, J. Phys. C: Solid State Phys. 10 (10) (1977) L271, http://dx.doi.org/10.1088/0022-3719/10/10/002.
[34] A. Liechtenstein, M. Katsnelson, V. Antropov, V. Gubanov, Local spin density functional approach to the theory of exchange interactions in ferromagnetic metals and alloys, J. Magn. Magn. Mater. 67 (1) (1987) 65–74, http://dx.doi.org/10.1016/0304-8853(87)90721-9.
[35] E.A. Stepanov, S. Brener, F. Krien, M. Harland, A.I. Lichtenstein, M.I. Katsnelson, Effective heisenberg model and exchange interaction for strongly correlated systems, Phys. Rev. Lett. 121 (2018) 037204, http://dx.doi.org/10.1103/PhysRevLett.121.037204.
[36] A. Posadas, M. Berg, H. Seo, A. de Lozanne, A.A. Demkov, D.J. Smith, A.P. Kirk, D. Zhernokletov, R.M. Wallace, Epitaxial integration of ferromagnetic correlated oxide $LaCoO_3$ with Si (100), Appl. Phys. Lett. 98 (5) (2011) 053104, http://dx.doi.org/10.1063/1.3549301.

[37] H. Seo, A. Posadas, A.A. Demkov, Strain-driven spin-state transition and superexchange interaction in $LaCoO_3$: *Ab* initio study, Phys. Rev. B 86 (2012) 014430, http://dx.doi.org/10.1103/PhysRevB.86.014430.

[38] K. Foyevtsova, J.T. Krogel, J. Kim, P.R.C. Kent, E. Dagotto, F.A. Reboredo, Ab initio quantum Monte Carlo calculations of spin superexchange in cuprates: The benchmarking case of Ca_2CuO_3, Phys. Rev. X 4 (2014) 031003, http://dx.doi.org/10.1103/PhysRevX.4.031003.

[39] V.A. Gavrichkov, S.I. Polukeev, S.G. Ovchinnikov, Cation spin and superexchange interaction in oxide materials below and above spin crossover under high pressure, Phys. Rev. B 101 (9) (2020) 094409, http://dx.doi.org/10.1103/physrevb.101.094409.

[40] S.G. Ovchinnikov, V.V. Val'kov, Hubbard Operators in the Theory of Strongly Correlated Electrons, Imperial College Press, London-Singapore, 2004.

[41] V.Y. Irkhin, Y.P. Irkhin, Many-electron operator approach in the solid state theory, Phys. Status Solidi (B) 183 (1) (1994) 9–58, http://dx.doi.org/10.1002/pssb.2221830102.

[42] V.Y. Irkhin, M.I. Katsnel'son, A.V. Trefilov, Electronic and lattice properties of high-T, superconductors due to the two-well potential for apex oxygen, J. Exp. Theor. Phys. 78 (6) (1994) 936–944, http://dx.doi.org/10.1002/pssb.2221830102.

[43] P. Werner, A.J. Millis, Efficient dynamical mean field simulation of the holstein-hubbard model, Phys. Rev. Lett. 99 (14) (2007) 146404, http://dx.doi.org/10.1103/physrevlett.99.146404.

[44] A. Sotnikov, J. Kunes, Field-induced exciton condensation in $LaCoO_3$, Sci. Rep. 6 (1) (2016) 30510, http://dx.doi.org/10.1038/srep30510.

[45] A. Fujii, T. Kondo, T. Taniguchi, T. Sakaiya, Neel transition in (Mg,Fe)O: A possible change of magnetic structure, Am. Mineral. 96 (2–3) (2011) 329–332, http://dx.doi.org/10.2138/am.2011.3534.

[46] J. Zaanen, G.A. Sawatzky, J.W. Allen, Band gaps and electronic structure of transition-metal compounds, Phys. Rev. Lett. 55 (4) (1985) 418–421, http://dx.doi.org/10.1103/physrevlett.55.418.

[47] S.G. Ovchinnikov, Effect of spin crossovers on the mott-hubbard transition at high pressures, J. Exp. Theor. Phys. 107 (1) (2008) 140–146, http://dx.doi.org/10.1134/s1063776108070145.

[48] A.G. Gavriliuk, V.V. Struzhkin, I.S. Lyubutin, S.G. Ovchinnikov, M.Y. Hu, P. Chow, Another mechanism for the insulator-metal transition observed in Mott insulators, Phys. Rev. B 77 (15) (2008) 155112, http://dx.doi.org/10.1103/physrevb.77.155112.

[49] S.G. Ovchinnikov, Analysis of the sequence of insulator-metal phase transitions at high pressure in systems with spin crossovers, J. Exp. Theor. Phys. 116 (1) (2013) 123–127, http://dx.doi.org/10.1134/s1063776113010111.

[50] C. Timm, C.J. Pye, Reentrant magnetic ordering and percolation in a spin-crossover system, Phys. Rev. B 77 (21) (2008) 214437, http://dx.doi.org/10.1103/physrevb.77.214437.

[51] Z. Ropka, R.J. Radwanski, 5D term origin of the excited triplet in $LaCoO_3$, Phys. Rev. B 67 (17) (2003) 172401, http://dx.doi.org/10.1103/physrevb.67.172401.

[52] A. Abragam, B. Bleaney, Electron Paramagnetic Resonance of Transition Ions, Clarendon, Oxford, 1970.

[53] A. Sotnikov, K.-H. Ahn, J. Kunes, Ferromagnetism of $LaCoO_3$ films, SciPost Phys. 8 (2020) 82, http://dx.doi.org/10.21468/SciPostPhys.8.6.082.

[54] H. Liu, J. Fan, F. Qian, Y. Ji, A. Rahman, R. Tang, L. Zhang, L. Ling, Y. Zhu, H. Yang, Two-dimensional magnetic interplay in the tensile-strained $LaCoO_3$ thin films, Phys. Chem. Chem. Phys. 23 (2021) 4912, http://dx.doi.org/10.1039/d0cp05550f.

[55] Y. Li, S.J. Peng, D.J. Wang, K.M. Wu, S.H. Wang, Strain effect on the magnetic and transport properties of $LaCoO_3$ thin films, AIP Adv. 8 (5) (2018) 056317, http://dx.doi.org/10.1063/1.5006280.

[56] N. Zhang, Y. Zhu, D. Li, D. Pan, Y. Tang, M. Han, J. Ma, B. Wu, Z. Zhang, X. Ma, Oxygen vacancy ordering modulation of magnetic anisotropy in strained $LaCoO_{3-x}$ thin films, ACS Appl. Mater. Interfaces 10 (44) (2018) 38230–38238, http://dx.doi.org/10.1021/acsami.8b13674.

[57] A.G. Gavriliuk, I. Trojan, I. Lyubutin, V. Sarkissian, S. Ovchinnikov, High-pressure magnetic properties and P–T phase diagram of iron borate, J. Exp. Theor. Phys. 100 (4) (2005) 688–696, http://dx.doi.org/10.1134/1.1926429.

[58] A.G. Gavriliuk, I.A. Trojan, S.G. Ovchinnikov, I.S. Lyubutin, V.A. Sarkisyan, The mechanism of suppression of strong electron correlations in $FeBO_3$ at high pressures, J. Exp. Theor. Phys. 99 (3) (2004) 566–573, http://dx.doi.org/10.1134/1.1809686.

[59] S. Beaulieu, S. Dong, N. Tancogne-Dejean, M. Dendzik, T. Pincelli, J. Maklar, R.P. Xian, M.A. Sentef, M. Wolf, A. Rubio, L. Rettig, R. Ernstorfer, Ultrafast dynamical lifshitz transition, Sci. Adv. 7 (17) (2021) eabd9275, http://dx.doi.org/10.1126/sciadv.abd9275.